Proceedings of the 17th World Congress
The International Federation of Automatic Control
Seoul, Korea, July 6-11, 2008

A Nonlinear Hybrid Fault Detection, Isolation and Estimation using Bank of Neural Parameter Estimators

E. Sobhani-Tehrani*, H. A. Talebi, and K. Khorasani*****

**Department of Electrical and Computer Engineering, Concordia University, Montreal, Quebec, H3G 1M8 CANADA (e-mail: e_sobhan@ ece.concordia.ca)*
*** Department of Electrical Engineering, Amirkabir University of Technology, Tehran, Iran (e-mail: htalebi@ece.concordia.ca)*
**** Department of Electrical and Computer Engineering, Concordia University, Montreal, Quebec, H3G 1M8 CANADA (e-mail: kash@ece.concordia.ca)*

Abstract: This paper presents two novel hybrid schemes for component fault diagnosis in a general nonlinear system. Unlike most fault diagnosis techniques, the proposed solution detects, isolates, and identifies the severity of faults in the system within a single integrated framework. The proposed technique is based on a bank of adaptive neural parameter estimators (NPE) and a set of parameterized fault models. At each instant of time, the NPEs provide estimates of the unknown fault parameters (FP) that are used for fault diagnosis. Two structures of NPE, namely series-parallel and parallel, are proposed with their respective fault isolation policies. While the series-parallel structure possesses fast convergence, the parallel scheme is extremely robust to measurement noise. Although, it has a more complex isolation policy, the parallel structure exhibits a more robust fault isolation capability. The parameter estimation for both architectures is based on an on-line minimization of instantaneous output estimation error. Simple network architecture and straightforward weight adaptation laws make our proposed technique appropriate for real-time implementation. Simulation results presented in this paper for detection, isolation, and identification of faults in nonlinear reaction wheel actuators of a 3-axis stabilized satellite in the presence of disturbances and noise demonstrate the effectiveness of our proposed fault diagnosis schemes.

1. INTRODUCTION

There is an increasing demand for man-made dynamical systems to operate autonomously in presence of faults and failures in sensors, actuators or components. Fault detection and identification is an essential component of an autonomous system. Hence, a high demand exists for development of intelligent systems that are able to autonomously detect the presence and isolate the location of faults occurring in different components of complex dynamical systems. On the other hand, accurate identification of fault severities is an invaluable asset for system maintenance operations (i.e. condition-based maintenance) as well as development of reliable autonomous recovery procedures. Furthermore, accurate estimation of severities in case of incipient faults allows system operators and controllers to intelligently plan and execute *a priori* pre-emptive actions to avoid catastrophic failures.

During the last two decades, a number of approaches have been developed for autonomous fault detection and isolation (FDI) of nonlinear systems. Most proposed techniques utilize either analytical model-based (Chen et al. 1999; Isermann 1994(a)) or expert system based methodologies (Patton et al. 1999; Rengaswamy et al. 2001; Sorsa et al. 1991; Korbicz et al. 1999). Only few works have been reported in the literature which simultaneously take advantage of mathematical model of a system, and adaptive nature of intelligent techniques especially neural networks, in a hybrid framework (Alessandri 2003; Xiaodong *et al.* 2002; Sobhani-Tehrani *et al.* 2005). However, many of these works either have not addressed the important problem of fault severity estimation (for example, Alessandri 2003) or have not provided a unified framework to simultaneously achieve FDI and fault severity estimation objectives.

The approach proposed in this paper essentially falls into a hybrid fault diagnosis framework. More specifically, mathematical model of the system is used as a basis for fault modeling. A variety of perspectives and concepts on fault modeling have been developed by different researchers in the field. For example, Polycarpou *et al.* (1995) have modeled faults as an unknown nonlinear function of system states and inputs. Patton *et al.* (1999) and Korbicz *et al.* (1999) have used dynamic neural networks to identify full system dynamics including nominal and faulty dynamics, under different fault scenarios. Furthermore, the notion of fault parameters (FP) was introduced in Alessandri (2003) to parameterize the mathematical model of a system with known structure but unknown parameters. The work proposed in this paper follows this perspective.

We design a *bank* of neural parameter estimators (NPE) to isolate faults. The idea of using a bank of estimators/observers/models has been previously proposed in the literature (Alessandri 2003; Rago *et al.* 1998; Medvedev 1998). However, they have neither addressed the problem of fault severity identification nor the issue of robustness to measurement noise, which considerably affects the performance of FDI algorithms in real-world applications. In this paper, a new integrated solution to the problem of nonlinear FDI and fault severity estimation is proposed. The proposed fault diagnosis methodology benefits from both *a priori* mathematical model information of the system and the adaptation capability of neural networks in a hybrid framework. Furthermore, two NPE structures, namely series-parallel and parallel, are proposed with their respective fault isolation policies, where each structure shows an exclusive set of desirable properties. For example, the proposed *parallel* scheme is extremely robust to measurement noise, hence making it suitable for low SNR applications. On the other hand, the series-parallel scheme displays very fast convergence rates that are desirable for systems requiring short delay in fault diagnosis. Thus, the choice of the appropriate FDI structure really depends on the characteristics and requirements of the specific problem at hand. Moreover, the neural networks architecture and the adaptation laws employed in both schemes are remarkably simpler than those employed by Alessandri (2003) and Sobhani-Tehrani *et al.* (2005), which makes the proposed methodology more suitable for real-time implementation.

2. PROBLEM FORMULATION AND FAULT MODELING

In this section, the problem of detecting and isolating faults in components of a general nonlinear system is formulated. Towards this end, consider a general nonlinear system described by the following nonlinear discrete-time state space representation:

$$\begin{aligned} x_{k+1} &= f(x_k, u_k) + d_k \\ y_k &= h(x_k) + n_k \end{aligned} \tag{1}$$

where $x_k \in \Re^n$ is the system state vector, $f : \Re^n \to \Re^n$, $h : \Re^n \to \Re^m$ are smooth vector functions on their respective domains, u_k is the control input vector, y_k is the system output vector, and d_k and n_k represent system disturbances and measurement noise, respectively. It is assumed that all system states are available for measurement. It is also assumed that disturbances and measurement noise are bounded signals, that is

$$\|d_k\| \le D_{\max} \ , \|n_k\| \le N_{\max} \quad \forall k \in N \tag{2}$$

Under full-state measurement assumption, the output equation in (1) can be redefined as $y_k = Cx_k$, where C is an $n \times n$ identity matrix.

Our objective is to design and develop a fault diagnosis scheme that is able to autonomously detect the presence, isolate the location, and identify the severity of faults in the system within a unified framework. We make the following assumptions regarding the occurrence of faults in the system, which comprise the basis for fault diagnosis design, development, and verification:

Assumption (i). The control input signals and the state vector remain bounded prior to and after the occurrence of a fault.

Assumption (ii). The faults take place at steady state operation of the system, which is a valid assumption for many practical systems.

Assumption (iii). The faults do not occur concurrently, i.e., at each instant of time only one fault might be present in the system.

Generally speaking, different models of a faulty system may be constructed. In this paper, following the work of Isermann (1994(b)), we have assumed that the system component faults are reflected in the physical system parameters. Thus, the presence of faults can be represented by changes in the parameters of the mathematical model of the system. Consequently, the faulty system can be described by the following parameterized nonlinear fault model, called multi-parameter fault model:

$$\Omega = \begin{cases} x_{k+1} = f(x_k, u_k, \alpha_k) + d_k \\ y_k = h(x_k) + n_k \end{cases} \tag{3}$$

where $\alpha_k \in \Re^L$ is the fault parameters (FP) vector containing L elements. Furthermore, $\alpha_k = \alpha_H$ implies the absence of faults in the system, i.e., healthy mode of operation. The value of α_H depends on the way that the FP vector affects the system model parameters in equation (3); being either additive or multiplicative. The representation adopted in this paper is the additive form, hence making $\alpha_H = [0]_{L\times 1}$.

The fault model (3) enables us to state the problem of nonlinear fault diagnosis in the form of an on-line nonlinear parameter estimation problem, where the unknown fault parameters are being estimated using system inputs and measurements.

3. FDI AND FAULT SEVERITY ESTIMATION

Within the proposed fault diagnosis framework, fault detection can be accomplished by simply comparing the estimated FP vector against α_H. However, for fault isolation and fault severity estimation purposes, we propose a bank of parameter estimators where each estimator is designed based on a fault model with single parameter.

Consider the multi-parameter fault model (3) with L fault parameters. One can extract L single-parameter models, $\Omega_i, i = 1,..., L$, from model (3) as follows:

$$\Omega_i : \begin{cases} x_{k+1} = f(x_k, u_k, \alpha_k^i) + d_k \\ y_k = h(x_k) + n_k \end{cases} ; i = 1,..., L \tag{4}$$

A bank of L parameter estimators may then be designed based on each separate fault model in (4), where the i^{th} parameter estimator will essentially estimate the i^{th} fault parameter.

Recursive Least Squares (RLS) is commonly used for parameter estimation of linear systems (Houacine 1992). Furthermore, Kalman filter (Haykin 2001) is the optimal parameter estimator under the hypotheses of Gaussian measurement and process noises and the linearity of state and measurement equations. For nonlinear systems, the Extended Kalman Filter (EKF) (Haykin 2001) is being extensively used as a standard technique for recursive estimation. However, it suffers from suboptimal performance and sometimes divergence due to errors introduced by the first-order approximation of the true nonlinear dynamics.

To overcome the above limitations and/or shortcomings, we choose multi-layer feed-forward (static) neural networks due to their excellent universal approximating properties and the availability of effective on-line adaptation algorithms. In this paper, we propose two neural parameter estimation schemes, namely "series-parallel" and "parallel" that differ mainly in their structure. This terminology is borrowed from system identification literature (Narendra *et al.* 1990; Abdollahi *et al.* 2006). It should be noted, however, that the idea of developing a bank of NPEs is entirely independent from the NPE architecture. Nonetheless, the fault isolation policy depends on the NPE structure being used, as will be shown in the following sections.

3.1 Series-Parallel Scheme

Fig. 1 depicts the structure of a bank of series-parallel NPEs designed and developed to simultaneously achieve the three objectives of fault detection, isolation, and fault severity estimation with minimum residual signal processing.

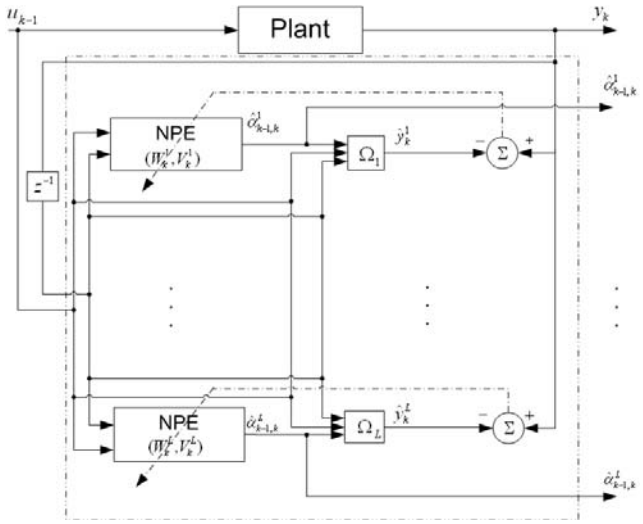

Fig. 1. Bank of series-parallel NPEs

NPE Calculations: The series-parallel structure is composed of two major subsystems including the nonlinear fault models given in (4) employed for state estimation, and feed-forward (static) neural networks utilized to adaptively approximate nonlinear FP estimation functions. Therefore, at each time-step k, two calculations are performed for each NPE of the bank as follows:

1) Calculation of FP estimates:

$$\hat{\alpha}^i_{k-1,k} = g\left(\bar{y}_k, W^i_k, V^i_k\right) \; ; \; i = 1,..., L \tag{5}$$

where $\hat{\alpha}^i_{k-1,k}$ is the estimate of the i^{th} fault parameter at time $k-1$ calculated at time k, W^i_k, V^i_k are the output and hidden layer weight matrices of the i^{th} NPE, respectively, $\bar{y}_k = \left[y_{k-1} \quad u_{k-1}\right]^{\mathrm{T}}$ is the input vector of *all* NPEs, and g is the nonlinear mapping implemented by the neural network and is defined as:

$$g\left(\bar{y}_k, W^i_k, V^i_k\right) = W^i_k \sigma\left(V^i_k \bar{y}_k\right) \tag{6}$$

where $\sigma(.)$ is the activation function of the hidden neurons that is usually considered as a sigmoidal function:

$$\sigma_j\left(V^i_k \bar{y}_k\right) = \frac{2}{1+\exp(-2V^i_{k_j}\bar{y}_k)} - 1 \tag{7}$$

where $V^i_{k_j}$ is the j^{th} row of V^i_k and $\sigma_j\left(V^i_k \bar{y}_k\right)$ is the j^{th} element of $\sigma\left(V^i_k \bar{y}_k\right)$.

2) State estimation (and subsequently output estimation) based on FP estimates:

$$\begin{cases} \hat{x}^i_k = f\left(x_{k-1}, u_{k-1}, \hat{\alpha}^i_{k-1,k}\right) \\ \hat{y}^i_k = \hat{x}^i_k \end{cases} ; i = 1,..., L \tag{8}$$

where $x_{k-1} = y_{k-1}$ are the measured states of the system.

Weight Update Laws: The weights of NPEs are updated with the objective of minimizing the weighted L_2 norm of the instantaneous output estimation error vector defined as:

$$\tilde{y}^i_k = y^i_k - \hat{y}^i_k \quad ; i = 1,..., L \tag{9}$$

Thus, the objective function, at time-step k, of the i^{th} NPE will be:

$$J^i_k = \frac{1}{2}\left\|\tilde{y}^i_k\right\|^2_Q = \frac{1}{2}\tilde{y}^{i\,\mathrm{T}}_k Q \tilde{y}^i_k \tag{10}$$

where $Q \in \Re^{n \times n}$ is the estimation error weight matrix.

The weights of NPEs are updated using the gradient descent (GD) algorithm as follows:

$$\begin{aligned} W^i_{k+1} &= W^i_k - \eta^i_w \left(\frac{\partial J^i_k}{\partial W^i_k}\right) \\ V^i_{k+1} &= V^i_k - \eta^i_v \left(\frac{\partial J^i_k}{\partial V^i_k}\right) \end{aligned} \quad ; i = 1,..., L \tag{11}$$

where $\eta_w^i, \eta_v^i > 0; i = 1,...,L$ are the learning rates. In order to derive the weight update laws, let us define:

$$net_{v_k}^i = V_k^i \bar{y}_k \tag{12}$$

$$net_{w_k}^i = W_k^i \sigma\left(V_k^i \bar{y}_k\right) \tag{13}$$

Thus, the partial derivatives $\partial J_k^i / \partial W_k^i$, $\partial J_k^i / \partial V_k^i$ can be computed according to the following equations:

$$\frac{\partial J_k^i}{\partial W_k^i} = \frac{\partial J_k^i}{\partial net_{w_k}^i} \frac{\partial net_{w_k}^i}{\partial W_k^i} \tag{14}$$

$$\frac{\partial J_k^i}{\partial V_k^i} = \frac{\partial J_k^i}{\partial net_{v_k}^i} \frac{\partial net_{v_k}^i}{\partial V_k^i} \tag{15}$$

where

$$\frac{\partial J_k^i}{\partial net_{w_k}^i} = \frac{\partial J_k^i}{\partial \tilde{y}_k^i} \frac{\partial \tilde{y}_k^i}{\partial \hat{y}_k^i} \frac{\partial \hat{y}_k^i}{\partial \hat{x}_k^i} \frac{\partial \hat{x}_k^i}{\partial \hat{\alpha}_{k-1,k}^i} \frac{\partial \hat{\alpha}_{k-1,k}^i}{\partial net_{w_k}^i} = -\tilde{y}_k^{i\mathrm{T}} Q \frac{\partial \hat{x}_k^i}{\partial \hat{\alpha}_{k-1,k}^i} \frac{\partial \hat{\alpha}_{k-1,k}^i}{\partial net_{w_k}^i} \tag{16}$$

$$\frac{\partial J_k^i}{\partial net_{v_k}^i} = \frac{\partial J_k^i}{\partial \tilde{y}_k^i} \frac{\partial \tilde{y}_k^i}{\partial \hat{y}_k^i} \frac{\partial \hat{y}_k^i}{\partial \hat{x}_k^i} \frac{\partial \hat{x}_k^i}{\partial \hat{\alpha}_{k-1,k}^i} \frac{\partial \hat{\alpha}_{k-1,k}^i}{\partial net_{v_k}^i} = -\tilde{y}_k^{i\mathrm{T}} Q \frac{\partial \hat{x}_k^i}{\partial \hat{\alpha}_{k-1,k}^i} \frac{\partial \hat{\alpha}_{k-1,k}^i}{\partial net_{v_k}^i} \tag{17}$$

$$\frac{\partial net_{w_k}^i}{\partial W_k^i} = \sigma\left(V_k^i \bar{y}_k\right), \frac{\partial net_{v_k}^i}{\partial V_k^i} = \bar{y}_k \tag{18}$$

The partial derivative $\partial \hat{x}_k^i / \partial \hat{\alpha}_{k-1,k}^i$ is calculated using the ith *state estimation* equation given in (8). Moreover, the standard back-propagation algorithm is used to calculate the partial derivatives $\partial \hat{\alpha}_{k-1,k}^i / \partial net_{w_k}^i$, $\partial \hat{\alpha}_{k-1,k}^i / \partial net_{v_k}^i$.

Isolation and Severity Policy: Given *Assumption (iii)*, the fault isolation policy for the series-parallel scheme is quite straight-forward and can be stated as follows:

$$\left(C, T_f\right) = \left\{ (i,k) \;\middle|\; \left| \hat{\alpha}_k^i - \alpha_H^i \right| > \varepsilon^i \right\} \tag{19}$$

where $\varepsilon^i; i = 1,...,L$ are the thresholds associated to each NPE in the bank, C specifies the index of the faulty component and T_f represents the detection time of the occurred fault. Once the fault source is isolated, the severity of the fault is essentially the value of the corresponding FP estimate. Fault isolation in series-parallel scheme is not perfect. Therefore, to augment its reliability, the thresholds in this scheme shall be selected in a way that a fault with a severity level below its respective threshold does not significantly deteriorate the closed-loop system performance.

3.2 Parallel Scheme

The series-parallel scheme developed in the previous section possesses several advantages including fast convergence and simple isolation policy. However, it can wrongly isolate faults specially when there is a strong coupling between two fault sources. Furthermore, it suffers from lack of robustness to measurement noise. This is due to the fact that measurement noise directly propagates through the network affecting the FP estimates, as can be observed in Fig. 1. The parallel scheme developed in this section will resolve both issues by feeding back the estimated rather than the measured outputs to the NPE input. Thus, the measurement noises are filtered out in the parallel scheme by the NPE adaptation process. Furthermore, using a special formulation of the fault isolation policy, the parallel scheme allows reliable and robust fault isolation. The schematic of the parallel structure is shown in Fig. 2.

Although the weight adaptation laws and NPE calculations for the parallel structure remain essentially very similar to the series-parallel approach, its isolation policy is substantially different. These changes are reflected in the following.

NPE Calculations and Update Laws: Since output estimations are used as feedback signals, y_{k-1} in (8) should be replaced by $\hat{y}_{k-1}^i$ for the ith NPE for $i = 1,...,L$. Similarly, $\hat{y}_{k-1}^i$ should be used in place of y_{k-1} in the input vector $\bar{y}_k$ of the NPEs, used in equations (5) and (18).

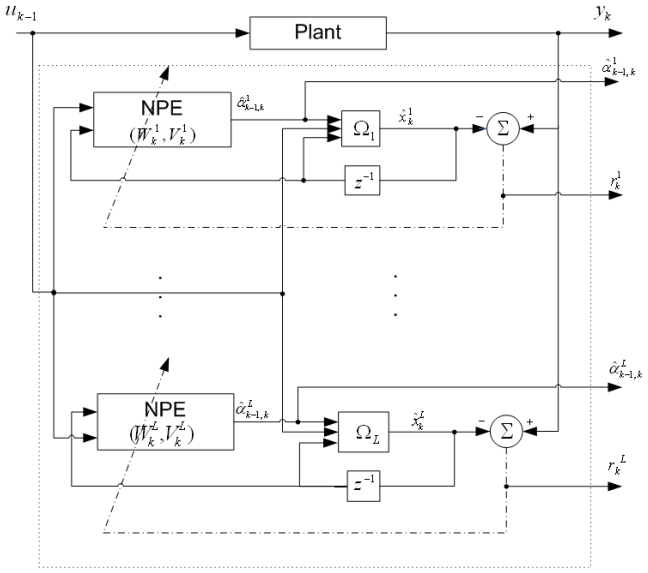

Fig. 2. Bank of parallel NPEs

Isolation and Severity Policy: To formulate the isolation policy, the *residual* vectors shall be introduced as:

$$r_k^i = y_k - \hat{y}_k^i \quad ; i = 1,...,L \tag{20}$$

Therefore, the isolation strategy can be stated as follows:

$$\left(C, T_f\right) = \left\{ (i,k) \;\middle|\; \left| r_k^{i,j} \right| \le \delta^{i,j} \; and \left| r_k^{l,j} \right| > \delta^{l,j}, l = 1,...,L, l \ne i, j = 1,...,n \right\} \tag{21}$$

where $r_k^{i,j}$ is the jth element of the residual vector r_k^i and $\delta^{i,j}$ is its corresponding *threshold*. The values of thresholds are determined using a worst-case disturbance analysis. Once the fault source is isolated, the severity of the fault is essentially the value of the corresponding FP estimate.

4. A CASE STUDY: APPLICATION TO FAULT DIAGNOSIS IN REACTION WHEEL ACTUATOR OF SATELLITE ACS

Fault diagnosis in Reaction Wheel actuators of Attitude Control Subsystem (ACS) of a 3-axis stabilized satellite is considered as a case study to evaluate the performance of the proposed fault diagnosis algorithms. Stringent requirements on satellites to operate autonomously in presence of faults in sensors, actuators and components together with inherent nonlinearity of reaction wheels and satellite attitude dynamics, make accurate and efficient fault diagnosis of ACS a challenging problem. Moreover, the number of reported publications (Al-Zyoud *et al.* 2006; Li *et al.* 2006; Talebi *et al.* 2006; Tudoroiu *et al.* 2005) on this topic over the recent years provides further evidence of the importance of the application.

To assess the performance of our proposed FDI techniques in a near-realistic environment, a highly accurate simulation model of a 3-axis stabilized satellite has been developed using MATLAB-Simulink. The simulation model consists of the well-known nonlinear satellite attitude dynamics (Chobotov 1991) where nonlinear Euler transformations are added to transform the satellite angular velocities to Euler angle rates, a high-fidelity nonlinear model of the reaction wheel (Bialke 1998) and a PID controller that stabilizes the closed-loop system so that *Assumption (i)* can be assured.

The model of a reaction wheel (RW) is given in the block diagram form in Fig. 3. The model incorporates all the nonlinearities as well as internal disturbances that are present in a real RW actuator. The closed-form nonlinear state-space representation of a reaction wheel model may be expressed as follows:

$$\begin{bmatrix}\dot{I}_m\\ \dot{\omega}\end{bmatrix}=\begin{bmatrix}G_d\omega_d[\psi_1(I_{bus},\omega)-\psi_3(\omega)]-\omega_d I_m\\ \frac{1}{J}[K_t I_m(1+B\varphi_1(\omega,t))-\tau_c\psi_2(\omega)-\tau_v\omega+C\varphi_2(\omega,t)]\end{bmatrix}+\begin{bmatrix}G_d\omega_d\\ 0\end{bmatrix}\mathrm{V_{Com}} \quad (22)$$

$$y=\begin{bmatrix}I_m\\ \omega\end{bmatrix}$$

where the current, I_m, and the angular velocity, ω, are the measured states of RW, $\mathrm{V_{Com}}$ is the input voltage signal of RW generated by the PID controller in the closed-loop attitude control system, ψ_1,ψ_2,ψ_3 are nonlinear functions modeling EMF torque limiting, coulomb friction, and speed limiter subsystems, respectively, I_{bus} is a highly nonlinear function of states and *bus voltage*, V_{bus}, and φ_1, φ_2 are representing torque ripple and cogging, respectively. Reaction wheel serves as the "plant" corresponding in Fig. 1 and Fig. 2 from the fault diagnosis design perspective. More precisely, the objective is to detect, isolate and estimate the severity of possible faults in the RW components using only the available wheel signals. Thus, measurements of RW current and angular velocity together with the wheel command voltage comprise the input vector of our proposed NPEs.

5. SIMULATION RESULTS

In this section, simulation results are presented to demonstrate the performance of our proposed FDI scheme. Simulations have been performed using nonlinear models of the reaction wheel and the attitude dynamics of a 3-axis stabilized satellite. Three decentralized PID controllers with gains $K_P=-100$, $K_I=-1$ and $K_D=-1000$ were used to stabilize the closed-loop system. The nonlinear model (22) was discretized using Euler backward difference method with sampling time of $T_s=0.05s$. The parameters of the reaction wheel were adopted from (Bialke 1998). Two three layer feed-forward neural networks with 4 neurons in the hidden layer and 1 neuron in the output layer are used as neural parameter estimators. Neural network parameters used for simulations are selected as $Q=\mathrm{I}_{2\times 2}$, $[\eta_w^{b1}\ \eta_v^{b1}]=[1\quad 10^{-4}]$ and $[\eta_w^{b2}\ \eta_v^{b2}]=[10^{-4}\quad 10^{-7}]$ for the first and the second NPE bank of the series-parallel scheme, respectively, and $\eta_w^{b1}=\eta_v^{b1}=0.7$ and $\eta_w^{b2}=\eta_v^{b2}=0.5\times 10^{-7}$ for the first and the second NPE bank of the parallel scheme.

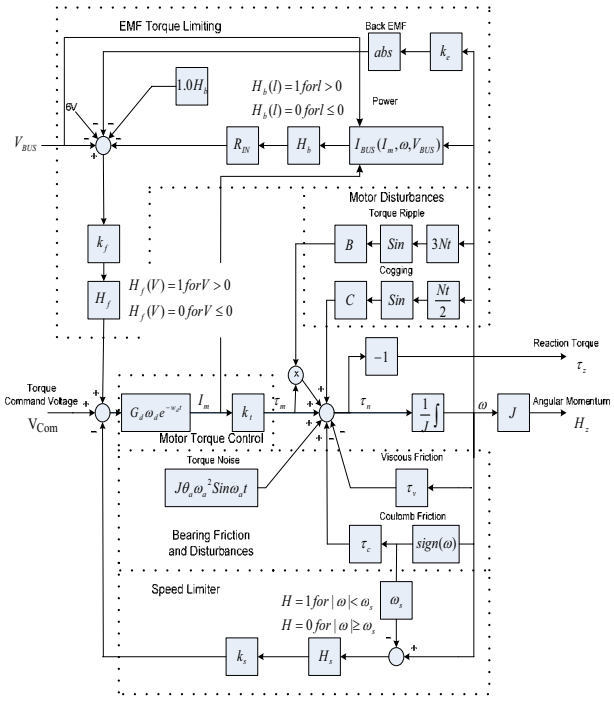

Fig. 3. Detailed reaction wheel (RW) block diagram (Bialke 1998)

A 20 degrees step reference was commanded to the satellite in the yaw channel. Random torque disturbance with the maximum magnitude of 10^{-4} N-m was acting on the satellite body. Since we are using reaction wheel state measurements, namely, wheel current and angular velocity, as inputs to our proposed fault diagnosis schemes, we have to design three copies of the same fault diagnosis subsystem for each reaction wheel on a 3-axis stabilized satellite. Thus, in order to avoid repetition, we have only shown the simulation results for one of the fault diagnosis subsystems. It should be noted that the results presented show the transient as well as the steady state operation of the system.

First, a series of intermittent faults with different severities were injected in the bus voltage, V_{bus}, over different time intervals as follows:

$$V_{bus}(t)=\begin{cases} V_{bus}^{nom}, & 0\le t<1000 \\ V_{bus}^{nom}-6, & 1000\le t<2240 \\ V_{bus}^{nom}-9.4, & 2240\le t<3100 \\ V_{bus}^{nom}-5.3, & 3100\le t<4390 \\ V_{bus}^{nom}-7.8, & 4390\le t<5100 \\ V_{bus}^{nom}, & 5100\le t\le 6000 \end{cases}$$

where V_{bus} is the value of the actual bus voltage and V_{bus}^{nom} is the value of bus voltage under healthy operational mode with the nominal value of 24V (Bialke 1998). The response of the series-parallel scheme is shown in Fig. 4. The actual angular velocity and the current of the reaction wheel and their estimates obtained from the first NPE bank are depicted in Figs. 4(a) and 4(b), respectively. These figures clearly show a very close match between the actual states and the corresponding estimates. Note also the effects of the fault on states of the reaction wheel. The fault parameter estimates obtained with low measurement noise are shown in Figs. 4(c) and 4(e) and those obtained by increasing the measurement noise by 10 times are shown in Figs. 4(d) and 4(f), respectively. It can be observed that under low measurement noise $\hat{\alpha}^1$ and $\hat{\alpha}^2$ approach to their true values very quickly, however, in presence of a large sensor noise the performance of the series-parallel scheme gets significantly deteriorated. More specifically, $\hat{\alpha}^1$ does not approach to its true value in the time period $t\in[5100\ \ 6000]$ and $\hat{\alpha}^2$ does wrongly exceed its threshold. Note that for the series-parallel scheme the thresholds required for fault isolation and severity policy are directly defined based on the fault parameters α_1,α_2 as $\varepsilon^1=1,\varepsilon^2=3\times10^{-3}$, respectively.

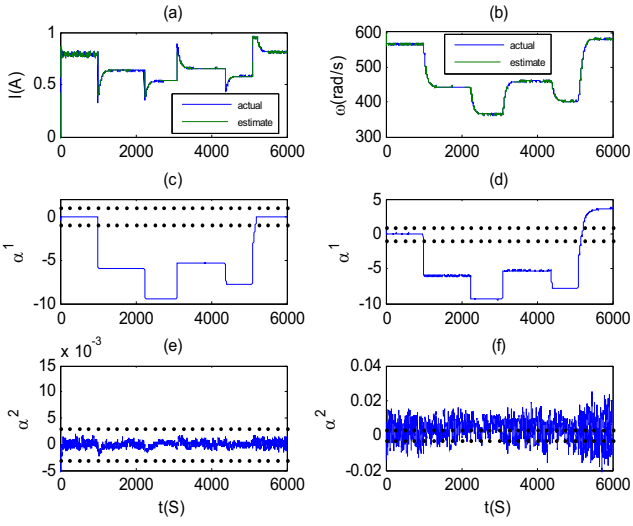

Fig. 4. The responses of the series-parallel scheme with a fault in Vbus

Next, the same command was given to the satellite and the following time varying fault was injected into the motor gain k_t at time $t=1000$:

$$k_t(t)=\begin{cases} k_t^{nom}, & t<1000 \\ k_t^{nom}+0.05\left[1+\sin\left(\dfrac{2\pi(t-1000)}{6000}-\dfrac{\pi}{2}\right)\right], & t>1000 \end{cases}$$

where k_t^{nom} is the nominal value of the motor gain under healthy operational mode that is equal to 0.029. The response of the series-parallel fault diagnosis scheme is shown in Fig. 5. The estimated angular velocity and the current obtained by the second NPE bank are depicted respectively in Fig. 5(a) and 5(b) together with their actual values. These figures reveal again that although the series-parallel scheme performs very well under low sensor noise conditions (i.e. the fault parameters converge very quickly to their actual values), it is not robust to measurement noise as evident by comparing Figs. 5(d) and 5(f) with Figs. 5(c) and 5(e), respectively. It can be easily observed in Fig. 5(d) that a 10 times increase in the measurements noise has caused the estimate of the bus voltage fault parameter, $\hat{\alpha}^1$, to wrongly exceed it threshold at time $t=5500(s)$. Furthermore, the accuracy of fault severity estimation for the motor gain fault has decreased considerably, as can be seen in Fig. 5(f).

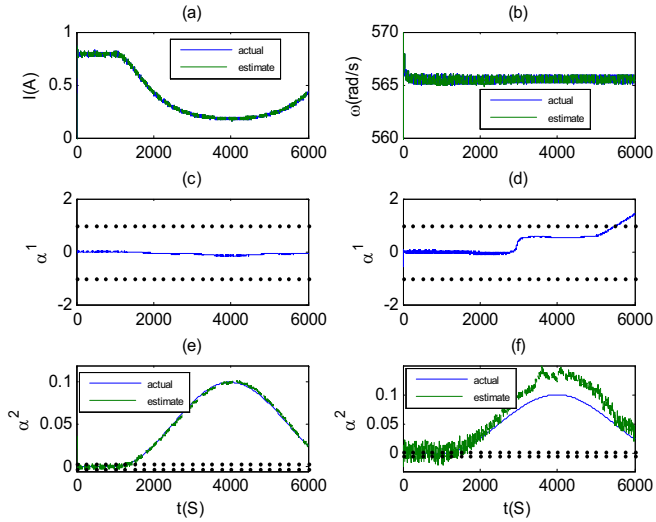

Fig. 5. The responses of the series-parallel scheme with a fault in the motor gain

Finally, the performance of the parallel structure is evaluated by using the same command and fault scenarios as in the case of the series-parallel scheme. The responses of the fault estimation scheme for faults in V_{bus} and k_t are shown in Figs. 6-9, respectively. Fig. 6(a), 6(c) and Figs. 8(a), 8(c) are obtained by using a low level sensor noise with faults in V_{bus} and k_t, respectively, whereas Figs. 6(b), 6(d) and Figs. 8(b) and 8(d) correspond to a high measurement noise conditions.

Comparing Fig. 6(a) with 6(b), and more specifically 8(c) with 8(d) show that the fault severity estimates in presence of large measurement noises have practically remained the same as the ones obtained under low sensor noise conditions. This reveals an excellent robustness property of the parallel scheme as compared to the series-parallel structure (see Figs. 5(c) and 5(d)).

Figs. 7 and 9 show the residuals generated for fault isolation policy as discussed in Section 3.2. In the parallel scheme the thresholds are defined for the residuals as opposed to the series-parallel scheme. The threshold values were selected based on the worst-case disturbance analysis as $\delta^{1,1} = \delta^{2,1} = 0.1(A)$ and $\delta^{1,2} = \delta^{2,2} = 15(rad/s)$ for the current and the angular velocity residuals, respectively.

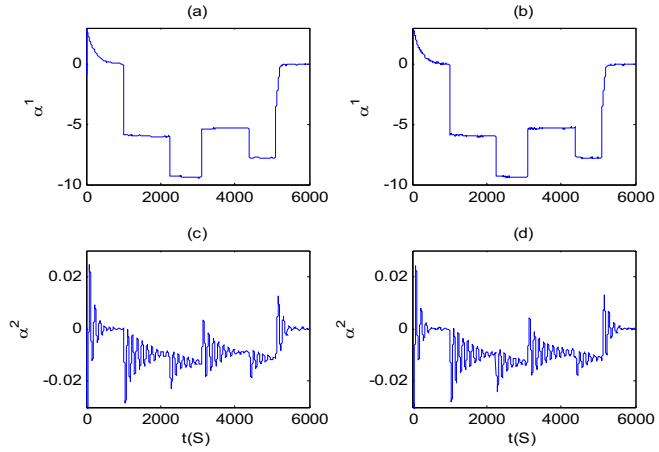

Fig. 6. The estimated fault parameters using the parallel scheme with a fault in Vbus

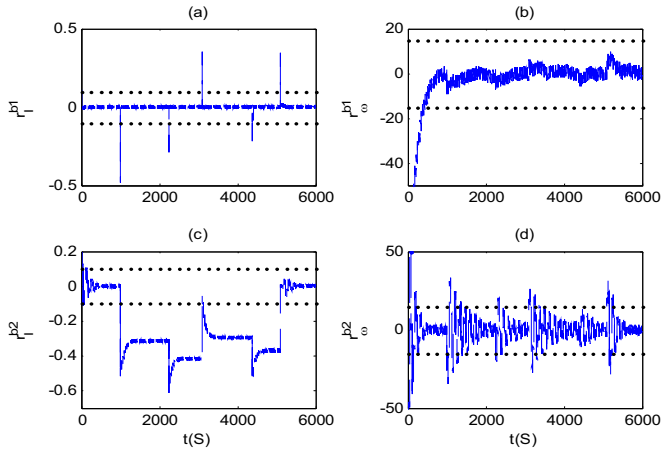

Fig. 7. The residual signals generated by the parallel scheme with a fault in Vbus

It can be observed that except for a short transient time, only the residuals generated by the first bank are within their specified thresholds in the presence of a fault in V_{bus} (see Figs. 7(a) and 7(b)) while at least one of the residuals associated to the second bank has exceeded its corresponding threshold. Therefore, the fault in V_{bus} has been isolated and the fault parameter estimates from the first bank will be taken as its severity estimate. Similarly, the fault in k_t results in the angular velocity residual of the first bank to exceed its corresponding threshold (see Fig. 9(b)) whereas the residuals of the second bank are both within their associated thresholds except for the transient period of the satellite's attitude maneuver (see Fig. 9(c) and 9(d)). Finally, comparing Fig. 5(e) to Fig. 8(c) reveals that the insensitivity/robustness of the parallel scheme with respect to measurement noise comes at the cost of slower convergence rate (i.e. longer transient phase) and a very small deterioration in the fault severity estimation accuracy when compared to the series-parallel scheme.

6. CONCLUSIONS

An integrated hybrid solution to the problem of fault detection, isolation, and fault severity identification in a general nonlinear system with full-state measurement was presented. The proposed approach is based on a bank of neural parameter estimators where each parameter is representative of a specific kind of system component fault. Two NPE schemes were proposed. While the series-parallel scheme enables straightforward FDI, relaxing the requirement of residual post-processing for fault isolation as commonly applied in standard approaches in the literature, the parallel approach is much more robust to measurement noise making it an appropriate choice for applications with small SNR measurements. Simulation results for fault diagnosis in reaction wheel actuators of the satellite's ACS confirm the advantages of each scheme.

The extension of our method to systems with partial state measurement has recently been achieved by the authors. The main remaining challenge that needs to be further investigated is the derivation of formal and analytical results on the performance of the fault diagnosis scheme and the NPEs, which is compounded due to nonlinearity of the problem, black-box nature of neural networks and the inherent coupling between estimation and adaptation of neural filters.

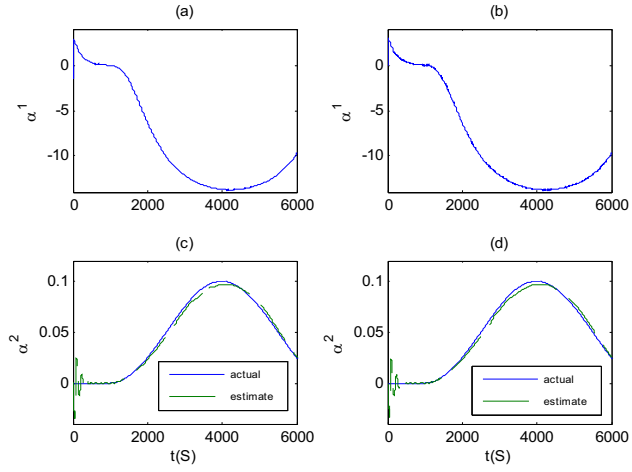

Fig. 8. The estimated fault parameters using the parallel scheme with a fault in motor gain

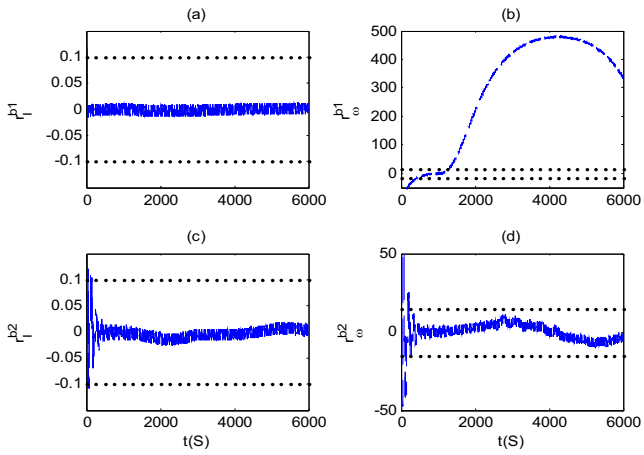

Fig. 9. The residual signals generated by the parallel scheme with a fault in motor gain

REFERENCES

F. Abdollahi, H.A. Talebi, R.V. Patel, "Stable identification of nonlinear systems using neural networks: Theory and experiments," *IEEE Transactions on Mechatronics*, vol. 11, No. 4, pp. 488 – 495, Aug 2006.

I. Al-Zyoud and K. Khorasani, "Neural network-based actuator fault diagnosis for attitude control subsystem of an unmanned space vehicle", *Proc. of the 2006 International Joint Conference on Neural Networks*, July 2006.

A. Alessandri, "Fault diagnosis for nonlinear systems using a bank of neural estimators," *Computers in industry*, vol. 52, pp. 271-289, 2003.

B. Bialke, "High fidelity mathematical modeling of reaction wheel performance," in 21st Annual American Astronautical Society Guidance and Control Conference, February 1998. AAS paper 98-063.

J. Chen and R. J. Patton, *Robust model based fault diagnosis for dynamic systems*, Kluwer Academic Publishers 1999, ISBN 0-7923-8411-3.

V. A. Chobotov, *Spacecraft attitude dynamics and control*, Malaber, FL: Kreiger, 1991.

S. Haykin, Kalman filters, in: S. Haykin (Ed.), *Kalman filtering and neural networks*, Wiley/Interscience, New York, pp. 1-22, 2001.

A. Houacine, "Regularized fast recursive-least squares algorithms for finite memory filtering," *IEEE Transactions on Signal Processing*, vol. 40, pp. 758-769, 1992.

R. Isermann, "Process fault detection and diagnosis methods," IFAC symposium SAFERPROCESS'94, Helsinki, Finland, vol.2, pp. 597-612, 1994 (a).

R. Isermann, "Fault diagnosis of machines via parameter estimation and knowledge processing - a tutorial paper," *Automatica*, vol. 29, No. 4, pp. 815-835, 1994 (b).

J. Korbicz, K. Patan and A. Obuchuwicz, "Dynamic neural networks for process modeling in fault detection and isolation systems," *Int. J. Applied Math. and Comp. Science*, vol. 9, no. 3, pp. 519-546, 1999.

Z. Q. Li, L. Ma, and K. Khorasani, "Dynamic neural network-based fault diagnosis for attitude control subsystem of a satellite," PRICAI 2006, LNAI 4099, pp. 308-318, Springer-Verlag, 2006.

A. Medvedev, "State estimation and fault detection by a bank of continuous finite-memory filters," *Int. J. Control*, vol. 69, No. 4, pp. 499-517, 1998.

K. S. Narendra and K. Parthasarathy, "Identification and control of dynamical systems using neural networks," *IEEE Trans. on Neural Networks*, vol. 1, no. 1, pp. 4-27, 1990.

R. J. Patton, C.J. Lopez-Toribio, and F. J. Uppal, "Artificial intelligence approaches to fault diagnosis," *IEE Colloquium on Condition Monitoring: Machinery, External Structures and Health* (Ref. No. 1999/034), pp. 5/I-5/18, April 1999.

M. M. Polycarpou. and A. J. Helmicki, "Automated fault detection and accommodation: a learning systems approach," *IEEE Trans. on Sys. Man Cybernetics*, vol. 25, no. 11, pp. 1447 – 1458, 1995.

C. Rago, R. Pransanth., R. K. Mehra and R. Fortenbaugh, "failure detection and identification and fault tolerant control using the IMM-KF with applications to the Eagle-Eye UAV," 37th IEEE Conf. on Decision and Control, vol. 4, pp. 4208-4213, 1998.

R. Rengaswamy, D. Mylaraswamy, V. Venkatasubramanian and K. E. Arzen, "A comparison of model-based and neural network-based diagnostic methods," *Engineering Applications of Artificial Intelligence*, vol. 14, pp. 808-818, 2001.

E. Sobhani-Tehrani, K. Khorasani, S. Tafazoli, "Dynamic neural network-based estimator for fault diagnosis in reaction wheel actuator of satellite attitude control system," Proc. Int. Joint Conf. on Neural Networks, pp. 2347-2352, 2005.

T. Sorsa, H. Koivo and H. Koivisto, "Neural networks in process fault diagnosis," *IEEE Trans. on Sys., Man and Cybernetics*, vol. 21, no. 4., pp. 815-825, 1991.

H. A. Talebi and R.V. Patel, "An intelligent fault detection and recovery scheme for reaction wheel actuator of satellite attitude control systems," IEEE Conf. on Control Applications, pp. 3282 – 3287, 2006.

N. Tudoroiu and K. Khorasani, "Fault detection and diagnosis for reaction wheels of satellite's attitude control system using a bank of Kalman filters," Int. Symp. on Signals, Circuits and Systems, vol. 1, pp. 199-202, 2005.

Z. Xiaodong, M. M. Polycarpou and T. Parisini, "A robust detection and isolation scheme for abrupt and incipient faults in nonlinear systems," *IEEE Trans. on Auto. Control*, vol. 47, no. 4, pp. 576 – 593, April 2002.